Thermalization component model of multiplicity distributions of charged hadrons measured at BNL ($E_{NN}^{\text{lab}} = 2$–11.6 GeV), at CERN ($E_{NN}^{\text{lab}} = 20$–200 GeV), and at BNL ($\sqrt{s_{NN}} = 19.6$–200 GeV)

Shengqin Feng[1,2] and Wei Xiong[1]

[1]*College of Science, China Three Gorges University, Yichang 443002, Hubei, People's Republic of China*

[2]*School of Physics and Technology, Wuhan University, Wuhan 430072, Hubei, People's Republic of China*

(Received 14 December 2007; published 23 April 2008)

We find that a collective flow model can successfully be used to analyze charged particle distributions at AGS and lower SPS (E_{NN}^{lab} less than 20 GeV in the laboratory frame) but fails at RHIC. The tail of the distribution of charged particles at RHIC has a jump from the collective flow model calculation as the energy increases. In this paper a thermalization component model is presented based on collective flow to study the multiplicity distributions at RHIC. It is realized that the region of phase space of collective flow can reflect that of the thermalization region. By comparing the contributions of particle production from the thermalization region at different energies and different centralities, we can deepen our study on collective movement at RHIC.

DOI: 10.1103/PhysRevC.77.044906 PACS number(s): 25.75.Ld, 25.75.Dw

I. INTRODUCTION

One of the central questions at the Relativistic Heavy-Ion Collider (RHIC) is the extent to which the quanta produced in collisions interact and thermalize [1,2]. Nuclear collisions generate enormous multiplicity and transverse energy, but to what extent does the collision generate matter in local equilibrium that can be characterized by the thermodynamic parameters temperature, pressure, and energy density? Only if thermalization has been established can more detailed questions be asked about the equation of state of the matter.

Recently, it was realized that the study of collective flow is one of the important tools for studying multihadron production of relativistic heavy-ion collisions [3,6,7]. This is because the longitudinal and transverse flows include rich physics, and collective flow relates closely to early evolution and nuclear stopping. Collective flow is often utilized to express the thermalization degree of relativistic heavy-ion collisions system. Detailed studies of the observed final-state flow pattern will deepen our understanding of the dynamic mechanism of relativistic heavy-ion collisions. Based on the pure thermal model, the collective flow model (CFM) [4,5] was developed. It achieves success in describing the charged particle distributions at AGS and lower SPS energies (20 GeV) and has become an indicator for the existence of collective flow at AGS [4,5]. But a detailed analysis of the experimental data at SPS and RHIC energies with CFM has shown that as the energy of collision is increased, the two tails of the charged hadron distributions have a symmetric jump away from the CFM calculation. This phenomenon has led us to reconsider collective flow theory at higher collision energy.

As shown in Fig. 1, CFM fails to analyze the charged hadron distribution at RHIC energy regions. As the collision energy increases, the tails of the distributions of experimental data deviate away from the calculation of CFM. The naive reason seems to be that experimental data on hadron yields are now available over a broad collision energy range at increasing collision energy. As the phase space of the particle distribution increases, thermalization throughout the entire phase space of particle production becomes more difficult. A detailed analysis of thermalization relation with centrality and energies at RHIC is needed.

The topic of this paper is how to simulate the data of charged hadron distributions at higher SPS and RHIC energy regions and to interpret what these results tell us. PHOBOS has used three Gaussian distributions to simulate the distribution of charged hadrons successfully [8–10,13]. Wolschin *et al.* [14] also discussed the charged hadron distribution by using three component distribution functions to construct the Fokker-Plank equation. Their models both assumed three random Gaussian distribution emitting sources. The three Gaussian sources represent target, projectile, and central source, respectively.

The main goal of this paper is to study the thermalization features of multiparticle production in heavy-ion collision at high energy in the framework of collective flow theory. We restrict ourselves here to the basic features and essential results of the CFM approach. A complete survey of the assumptions and results, as well as of the relevant references, is available in Refs. [4,5,15,17–20].

The paper is organized as follows. The analysis details based on the thermalization component model (TCM) are described in Sec. I. The comparisons of TCM calculations with experimental data and the related theoretical analysis with TCM are given in Sec. III. A summary is given in Sec. IV.

II. THERMALIZATION COMPONENT MODEL

The hot and dense matter produced in relativistic heavy-ion collisions may evolve through the following scenario: pre-equilibrium, thermal (or chemical) equilibrium of partons, possible formation QGP or a QGP hadron gas mixed state, a gas of hot interacting hadrons, and, finally, a freeze-out state when the produced hadrons no longer strongly interact with each other. Since the produced hadrons carry information about the collision dynamics and the entire space-time evolution of the system from the initial to the final stage of collisions, a precise analysis of the multiplicity distributions of charged hadrons is

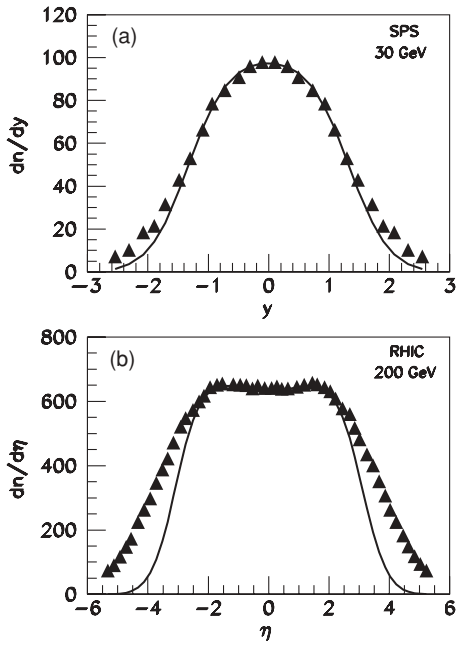

FIG. 1. (a) π meson rapidity distribution of $E_{NN}^{\rm lab} = 30$ GeV at SPS [7]; (b) charged hadron pseudo-rapidity distribution of $\sqrt{s_{NN}} = 200$ GeV.

essential for the understanding of the dynamics and properties of the created matter.

A detailed analysis of the experimental data at SPS and RHIC energy with CFM has shown that, as the collision energy is increased, the two tails of the π or the charged hadron distributions show a (symmetric) discrepancy between the data and the calculation. This phenomenon has led us to reconsider collective flow theory at higher collision energy. A detailed analysis of the relation among thermalization, centralities, and energies at RHIC is needed. Let us first sketch our overall picture and detail our arguments subsequently. The model we considered contains three distinct assumptions, some of which are rather different from those usually contained in other flow models.

(i) The size of the phase space of the particle distribution increases with the increase of collision energy. It seems more difficult to achieve thermalization throughout the entire phase space of particle production at SPS and RHIC energies. It is assumed that a Gaussian distributions fits the distributions of the produced charged hadrons at the two fragmentation regions, and thermalization prefers to occur at the central rapidity region at SPS and RHIC.

(ii) The collective flow of the central rapidity region carries information of the early time of heavy-ion collision. The system expands not only in the longitudinal direction but also in the transverse direction. A two-dimensional collective flow is used to study the thermalization process at RHIC.

(iii) The phase space is compartmentalized into two regions: a thermalization region and a nonthermalization region. The nonthermalization region is located at the two fragmentation regions. The total multiplicity distribution is the sum of the contributions from the target fragmentation region, the projectile fragmentation region, and the central region, respectively:

$$\frac{dN}{dy} = N_1 F_1 + N_2 F_2 + N_3 F_3 = \sum_i N_i F_i, \qquad (1)$$

where $i = 1$, 2, and 3 denotes target, projectile, and central region, respectively, and N_i and F_i are the particle numbers and the normalization functions, respectively, of target, projectile, and central regions.

As assumed before, the distributions of target and projectile fragmentation regions are given with Gaussian distributions:

$$F_1 = \frac{1}{\sqrt{2\pi}\sigma} e^{-\frac{(y+y_1)^2}{2\sigma^2}}, \qquad (2)$$

$$F_2 = \frac{1}{\sqrt{2\pi}\sigma} e^{-\frac{(y+y_2)^2}{2\sigma^2}}, \qquad (3)$$

where σ is the distribution width of the Gaussian and y_1, y_2 are the locations of central of target and projectile-emitting source.

F_3 is the distribution of two-dimensional flow, which is given by [4,5]

$$F_3 = \frac{g\tau_f R_f^2 K}{8\pi} \int_{m_t^{\rm lo}}^{m_t^{\rm hi}} dm_t^2 m_t I_0(\alpha) \times \int_{-\eta_0}^{-\eta_0} d\eta_l \cosh(y-\eta_l) e^{\mu/T} e^{-\tilde{\alpha}\cosh(y-\eta_l)}, \qquad (4)$$

where $m_t^{\rm lo}$ and $m_t^{\rm hi}$ are the experimental limits in which the spectrum is measured, the freeze-out radius R_f and the longitudinal extent of the fireball are fixed via the finite interval $(-\eta_0, \eta_0)$, and I_0 is modified Bessel function.

We should say a few words about two-dimensional flow theories. The geometry of the freeze-out of a fixed two-dimensional flow hypersurface σ_f is as follows: In the time direction we take a surface of constant proper time. In the η_l direction, the freeze-out volume extends only to a maximum space-time rapidity η_0, which is required by the finite available total energy and breaks longitudinal boost-invariance, as proposed by Bjorken [16]. In the transverse direction the boundary is given by R_f, which describes a cylindrical fireball in η-r space. A detailed discussion is presented in Refs. [4,5].

III. COMPARISONS WITH EXPERIMENTAL DATA

It is found that CFM describes the experimental data of charged particle distributions very well when we discuss Au-Au center collisions at the AGS energy region. The contribution of the fragmentation regions can be ignored, so Eq. (1) can be simplified to

$$\frac{dN}{dy} = N_3 F_3. \qquad (5)$$

The results from CFM are consistent with experimental data in Au-Au collisions at the AGS energy region ($E_{NN}^{\rm lab} =$

2, 4, 6, 8, and 11.6 GeV in the laboratory frame). This indicates that when at the lower AGS energy region CFM can describe the charged particle distribution well, and so our TCM reverts to the CFM. The reason seems to be that phase space is small and the nucleus stopping power is very strong at the AGS energy region, so particles can be almost completely thermalized throughout the entire phase space. The same situation is true for the SPS energy region below 20 GeV.

However, as the collision energies increase (E_{NN}^{lab} above 30 GeV), the experimental points make a symmetric jump away from the of CFM calculation at the two tails (as shown in Fig. 1). This phenomenon can be explained by the nuclei's penetrability. The higher the collision energies, the more transparent the nuclei, and the larger the extension of the phase space of the produced particle. Collective flow is formed at the central rapidity region after thermalization. The distributions of nonthermalized charged hadrons are represented by a Gaussian. The thermalization area becomes one part of the whole phase space.

Since June 2000, RHIC has opened a new energy region for the study of multihardon production. We have analyzed the experimental data of charged particle distributions in Au-Au center collisions in the RHIC energy region from 19.6 to 200 GeV of $\sqrt{s_{NN}}$.

We can calculate the rapidity distribution of charged particles with Eq. (1). It is known that we can transfer the rapidity distribution to a pseudo-rapidity distribution just by multiplying by a factor [21]:

$$\frac{dN}{d\eta} = \frac{dN}{dy}\sqrt{1-\left(\frac{m}{m_T\cosh y}\right)^2}. \tag{6}$$

We fit the experimental data of the RHIC energy region by TCM with χ^2/dof. The comparison of the measured and calculated distributions for the best fit (χ^2/dof minimization) is presented in Fig. 2. The TCM calculations are accordant with the experimental data shown in Fig. 2. The percentages found by the TCM of the charged hadron production from the thermalization regions in the AGS, SPS, and RHIC energy regions are presented in Fig. 3. It is found that most of the produced particles at AGS come from the thermalization region, and the percentage of produced particles from the thermalization region decreases as the energy increases. This

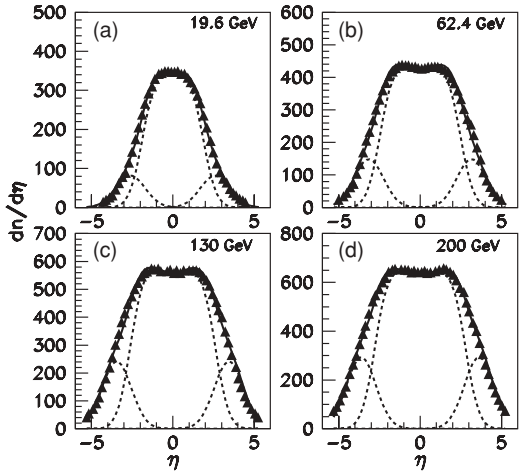

FIG. 2. The pseudo-rapidity distributions at $\sqrt{s_{NN}} =$ 19.6, 62.4, 130, and 200 GeV for Au + Au collisions. Experimental data are given by triangles [8–10]. The solid lines are the results given by TCM, which is the summation of the three component contributions.

trend becomes weaker and seems to reach saturation as $\sqrt{s_{NN}}$ reaches 62.4 GeV at the RHIC energy region. The detailed fit parameters of our TCM with experimental data are shown in Table I.

The PHOBOS Collaboration, working at RHIC, has presented considerable experimental data [8–10] of different energies and different centralities, including Au + Au collisions and Cu + Cu collisions at $\sqrt{s_{NN}} = 62.4$ and 200 GeV. It is found that the calculation results from TCM are consistent with those of the experimental data. The results are presented in Fig. 4 and Table I. The experimental data are taken from Refs. [8–13].

It is shown in Fig. 5 that the percentage ratios of the particle production from the thermalization regions increase with the increase of the centralities at RHIC. From Fig. 5(a), it is seen that the contribution ratios from the thermalization region is appreciably larger for the smaller collision system (Cu + Cu) than for the larger collision system (Au + Au) at $\sqrt{s_{NN}} =$ 62.4 GeV. But from Fig. 5(b), we find that the percentage ratios of particle production from thermalization regions is

TABLE I. The fit results of TCM with the experimental data at SPS and RHIC energy regions.

	E_{NN}^{lab}	η_0	$y_{1,2}$	n_1+n_2	n_3	$n_3/(n_1+n_2+n_3)$
	30	1.33	±2.1	16	256	94.13%
	40	1.4	±2.05	22	301	93.19%
	80	1.4	±2.0	64	392	85.97%
SPS	158	1.38	±2.0	100	507	83.52%
	$\sqrt{s_{NN}}$	η_0	$y_{1,2}$	n_1+n_2	n_3	$n_3/(n_1+n_2+n_3)$
	19.6	1.85	±2.6	370	1310	77.99%
	62.4	2.47	±3.15	670	2157	76.30%
	130	2.62	±3.45	1100	3016	73.28%
RHIC	200	2.8	±3.62	1320	3629	73.38%

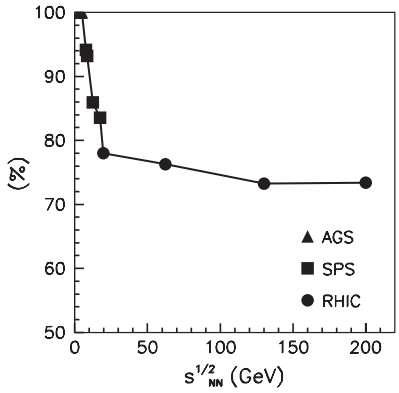

FIG. 3. The dependence of the percentage of the charged hadron production from the thermalization regions on the collision energy.

almost independent of the size of collision systems at $\sqrt{s_{NN}} =$ 200 GeV.

In our TCM, the free parameters are the limitation of collective flow η_0 and the emission sources' positions in the fragmentation area, $y_{1,2}$. We have $y_1 = -y_2$ in the case of symmetrical collisions. The values for transverse flow and temperature of collective flow refer to those in Refs. [4,5,15,20]. The values of $n_i (i = 1, 2, 3)$ are numbers of particles from the fragmentation and the thermalization regions. respectively.

A linear relationship is obtained between η_0 and $\ln \sqrt{s_{NN}}$ by detailed study (see Fig. 6). The linear equations are given by fitting four data points at SPS and RHIC energy regions as follows:

$$\eta_0 = 0.40 \ln \sqrt{s_{NN}} + 0.71, \tag{7}$$

where η_0 is the extension of collective flow. From Eq. (7), we can predict the extension of the thermalization region at LHC with increasing collision energy.

Here, we should mention that quite a few theoretical models can give equally good representation of the data of particle productions at AGS, SPS, and RHIC, including thermal

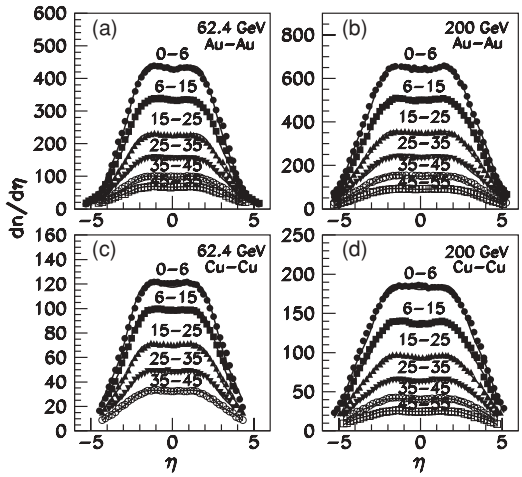

FIG. 4. The charged hadron pseudo-rapidity distribution at different centrality at $\sqrt{s_{NN}} = 62.4$ and 200 GeV for Au + Au and Cu + Cu collisions, respectively. Solid lines are the results from TCM, Experimental data are given by PHOBOS [8–13].

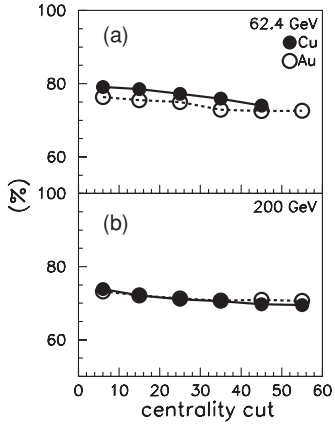

FIG. 5. The dependence of the percentage from the thermalization region on different centralities for $\sqrt{s_{NN}} = 62.4$ and 200 GeV.

models [22–25] based on the assumption of global thermal and chemical equilibrium, hydrodynamic models [26–31] based only on the assumption of local thermal equilibrium, and transport models [32–37] that treat nonequilibrium dynamics explicitly. The thermal models have been very successful in accounting for the yield of various particles and their ratios, whereas the hydrodynamic models are particularly useful for understanding the collective behavior of low-transverse-momentum particles such as in the elliptic flow. Since transport models treat chemical and thermal freeze-out dynamically, they are also natural and powerful tools for studying the Hanbury-Brown-Twiss interferometry of hadrons.

For hard processes that involve large momentum transfer, approaches based on perturbative quantum chromodynamics (pQCD) using parton distribution functions in the colliding nuclei have been used [38]. Also, the classical Yang-Mills theory has been developed to address the evolution of parton distribution functions in nuclei at ultra-relativistic energies and used to study the hadron rapidity distribution and its centrality dependence at RHIC [39–41]. These problems have also been studied in the pQCD-based final-state saturation model [42–44]. A multiphase transport (AMPT) model that includes both initial partonic and final hadronic interactions and the transition between these two phases of matter [45–48] was constructed to describe nuclear collisions ranging from p-A to A-A systems at center-of-mass energies from about $\sqrt{s_{NN}} = 5$ to 5500 GeV at LHC.

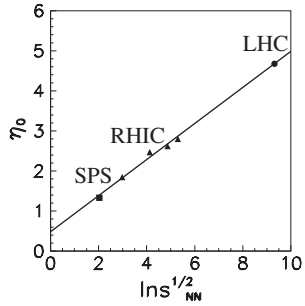

FIG. 6. The relation between the limitation of thermalization region with $\ln \sqrt{s_{NN}}$.

IV. SUMMARY AND CONCLUSIONS

Hadron multiplicities and their distributions are observables that can provide information on the nature, composition, and size of the medium from which they originate. Of particular interest is the extent to which the measured particle yields show thermalization. The feature of thermalization of high-energy heavy-ion collisions at RHIC has been analyzed in this paper.

CFM fails to analyze the charged particle distributions when the collision energies increase to above 30 GeV. The tail of the distribution of the charged particles at RHIC jumps from the CFM calculation as the energy increases. The naive reason seems to be that the experimental data on hadron yields are now available over a broad collision energy range with the increase of collision energy. It seems more difficult for achieve thermalization throughout the entire phase space of particle production with the increase of the phase space of the particle distribution.

However, the phenomena may suggest that something else happens, such as the onset of deconfinement in the early stage of the reaction with the collision energy (E_{NN}^{lab}) above 30 GeV in the laboratory frame, which has been mentioned in Ref. [49]. In Ref. [49], central Pb-Pb collisions were studied in the SPS energy range. At around $E_{NN}^{\text{lab}} = 30$ GeV the ratio of strangeness to pion production shows a sharp maximum, the rate of increase of the produced pion multiplicity per wounded nucleon increases, and the effective temperature of pions and kaons levels off to a constant value. These features are not reproduced by present hadronic models; however, there is a natural explanation in a reaction scenario with the onset of deconfinement in the early stage of the reaction at SPS energy.

Collective flow in heavy-ion collisions is an unavoidable consequence of thermalization. The extension of the phase space of collective flow can reflect that of the thermalization region. It is found that the TCM can fit the experimental data well for particle production throughout the whole AGS, SPS, and RHIC energy regions. The percentage ratios of contributions of the particle production from the thermalization region are the largest at AGS and decrease as collision energies increase at SPS and RHIC, but they seem to reach saturation when $\sqrt{s_{NN}} = 62.4$–200 GeV at RHIC. It is also found that the extension of the flow shows a linear dependence on $\ln \sqrt{s_{NN}}$. From that, we can predict the thermalization extension for future LHC experimental data.

It is shown from our study that the percentage ratios of particle production from thermalization regions increase with the increase of the centralities at RHIC. The contribution ratios from the thermalization region are appreciably larger for the smaller collision system (Cu + Cu) at $\sqrt{s_{NN}} = 62.4$ GeV but are independent of the collision system at $\sqrt{s_{NN}} = 200$ GeV.

ACKNOWLEDGMENTS

The authors are indebted to Prof. Lianshou Liu for many valuable discussions and very helpful suggestions. This work was supported by the Excellent Youth Foundation of Hubei Scientific Committee (2006ABB036) and Natural Science Foundation of China Three Gorges University (2003C02).

[1] P. Jacobs and X. N. Wang, Prog. Part. Nucl. Phys. **54**, 443 (2005).
[2] A. H. Mueller, Nucl. Phys. **B572**, 227 (2000).
[3] U. Mayer and U. Heinz, Phys. Rev. C **56**, 439 (1997); E. Schnedermann and U. Heinz, Phys. Rev. C **50**, 1675 (1994); U. Heinz, Nucl. Phys. **A661**, 140c (1999).
[4] E. Schnedermann, J. Sollfrank, and U. Heinz, Phys. Rev. C **48**, 2462 (1993).
[5] E. Schnedermann and U. Heinz, Phys. Rev. C **47**, 1738 (1993).
[6] P. Braun-Munzinger, J. Stachel, J. P. Wessels, and N. Xu, Phys. Lett. **B344**, 43 (1995); P. Braun-Munzinger, J. Stachel, J. P. Wessels, and N. Xu, Phys. Lett. **B365**, 1 (1996); P. Braun-Munzinger and J. Stachel, Nucl. Phys. **A606**, 320 (1996).
[7] C. Blume, Acta Phys. Hung. A **24**, 31 (2005).
[8] B. B. Back *et al*., Phys. Rev. Lett. **93**, 082301 (2004).
[9] B. B. Back *et al*., Phys. Rev. C **74**, 021901 (2006).
[10] B. B. Back *et al*., Phys. Rev. Lett. **87**, 102303 (2001).
[11] I. G. Bearden *et al*., Phys. Rev. Lett. **88**, 202301 (2002).
[12] G. Roland *et al*., J. Phys. G **30**, S1133 (2004).
[13] J. Alexandru, Acta Phys. Hung. A **22**, 121 (2005).
[14] G. Wolschin, Eur. Phys. J. A **5**, 85 (1999).
[15] S. Feng, *Introduction to Multi-hadron Productions at High Energy Heavy-Ion Collisions* (Beijing Institute of Technology Press, Beijing, 2005) [in Chinese].
[16] J. D. Bjorken, Phys. Rev. D **27**, 140 (1983).
[17] S. Feng, F. Liu, and L. Liu, Phys. Rev. C **63**, 014901 (2000).
[18] S. Feng, F. Liu, and L. Liu, High Energy Phys. Nucl. Phys. **26**, 1277 (2002) [in Chinese].
[19] S. Feng, X. Yuan, and Y. Shi, Mod. Phys. Lett. A **21**, 663 (2006).
[20] X. Yuan and S. Feng, High Energy Phys. Nucl. Phys. **29**, 371 (2005) [in Chinese].
[21] C.-Y. Wong, *Introduction to High-Energy Heavy-Ion Collisions* (World Scientific Publishing, Singapore, 1994).
[22] P. Braun-Munzinger, J. Stachel, J. P. Wessels, and N. Xu, Phys. Lett. **B344**, 43 (1995).
[23] P. Braun-Munzinger, I. Heppe, and J. Stachel, Phys. Lett. **B465**, 15 (1999).
[24] F. Becattini, J. Cleymans, A. Keranen, E. Suhonen, and K. Redlich, Phys. Rev. C **64**, 024901 (2001).
[25] J. Cleymans and K. Redlich, Phys. Rev. Lett. **81**, 5284 (1998).
[26] D. H. Rischke, S. Bernard, and J. A. Maruhn, Nucl. Phys. **A595**, 346 (1995).
[27] D. H. Rischke, Y. Pursun, and J. A. Maruhn, Nucl. Phys. **A595**, 383 (1995); **A596**, 717(E) (1996).
[28] C. M. Hung and E. V. Shuryak, Phys. Rev. Lett. **75**, 4003 (1995).
[29] P. Huovinen, P. F. Kolb, U. W. Heinz, P. V. Ruuskanen, and S. A. Voloshin, Phys. Lett. **B503**, 58 (2001).
[30] P. F. Kolb, P. Huovinen, U. W. Heinz, and H. Heiselberg, Phys. Lett. **B500**, 232 (2001).
[31] P. F. Kolb, U. W. Heinz, P. Huovinen, K. J. Eskola, and K. Tuominen, Nucl. Phys. **A696**, 197 (2001).
[32] H. Sorge, Phys. Rev. C **52**, 3291 (1995).
[33] S. A. Bass *et al*., Prog. Part. Nucl. Phys. **41**, 225 (1998).
[34] D. Molnar and M. Gyulassy, Phys. Rev. C **62**, 054907 (2000).

[35] D. E. Kahana and S. H. Kahana, Phys. Rev. C **63**, 031901(R) (2001).
[36] B. Li, A. T. Sustich, B. Zhang, and C. M. Ko, Int. J. Mod. Phys. E **10**, 267 (2001).
[37] B. H. Sa, X. Cai, Z. D. Su, A. Tai, and D. M. Zhou, Phys. Rev. C **66**, 044902 (2002).
[38] X. N. Wang, Phys. Rep. **280**, 287 (1997).
[39] D. Kharzeev and E. Levin, Phys. Lett. **B523**, 79 (2001).
[40] D. Kharzeev, E. Levin, and M. Nardi, Nucl. Phys. **A730**, 448 (2004); **A743**, 329(E) (2004).
[41] D. Kharzeev and M. Nardi, Phys. Lett. **B507**, 121 (2001).
[42] K. J. Eskola, K. Kajantie, P. V. Ruuskanen, and K. Tuominen, Nucl. Phys. **B570**, 379 (2000).
[43] K. J. Eskola, K. Kajantie, and K. Tuominen, Phys. Lett. **B497**, 39 (2001).
[44] K. J. Eskola, K. Kajantie, P. V. Ruuskanen, and K. Tuominen, Phys. Lett. **B543**, 208 (2002).
[45] Z. W. Lin, C. M. Ko, and S. Pal, Phys. Rev. Lett. **89**, 152301 (2002).
[46] Z. W. Lin and C. M. Ko, Phys. Rev. C **68**, 054904 (2003).
[47] Z. W. Lin and C. M. Ko, J. Phys. G **30**, S263 (2004).
[48] Z. W. Lin, C. M. Ko, B. A. Li, B. Zhang, and S. Pal, Phys. Rev. C **72**, 064901 (2005).
[49] S. V. Afanasiev *et al*., Phys. Rev. C **66**, 054902 (2002).